

Review Article

Pressure Broadening of Some He I Lines

Banaz Omar

Physics Department, Research Center OPTIMAS, Technical University of Kaiserslautern, Erwin Schroedinger Str. 46, 67663 Kaiserslautern, Germany

Correspondence should be addressed to Banaz Omar, omar@rhrk.uni-kl.de

Received 29 April 2009; Accepted 12 July 2009

Academic Editor: Roland Stamm

Copyright © 2010 Banaz Omar. This is an open access article distributed under the Creative Commons Attribution License, which permits unrestricted use, distribution, and reproduction in any medium, provided the original work is properly cited.

Quantum statistical approach is adopted for calculating the spectral line shapes of neutral helium in dense plasmas. Stark broadening of isolated He I lines 5048 Å ($2^1P - 4^1S$), 3889 Å ($2^3S - 3^3P$), and 3188 Å ($2^3S - 4^3P$) is presented. Based on thermodynamic Green's function, the electronic contribution to the shift and width is considered. The participation of ions to the line broadening is treated in a quasistatic approximation, by taking both quadratic Stark effect and quadrupole interaction into account. The calculated shifts and widths are compared with existing data.

1. Introduction

Plasma spectroscopy deals with the characteristics of radiation emitted from a plasma. In dense plasmas, damping of the emitted radiation occurs by means of several mechanisms; the most effective one is pressure broadening (Stark broadening). The interaction between a radiating atom and surrounding perturbing particles leads to Stark broadening. High-speed electrons perturb the emitter by collisions, causing the interruption of the spontaneous emission and altering the emitter energy levels [1–4].

Line profile calculation is an interesting tool for both laboratory and astrophysical plasma diagnostics, for example, to determine the internal parameters, to understand the microscopic processes within the plasma, and to check the quality of the predicted experimental and theoretical parameters [1, 2].

The emission spectra of helium and He-like ions with their simple atomic structures are interesting for plasma diagnostics such as in shock wave tube or pulsed arc plasmas [5, 6] and in the astrophysical context, for example, stellar atmospheres of hot stars and white dwarfs [7–9]. Helium is used as a carrier gas in many laboratories and is weekly interacting with materials and less harmful for plasma facing components than hydrogen and its isotopes [5]. The He-like ions may exist even at extremely high temperatures and densities. Even ITER is started with helium discharge, also He can be observed in discharge of JET. Spectroscopic

measurements of tokamak plasmas are not free from helium [10].

Various approaches have been investigated to calculate spectral line shapes in plasmas [9, 11–24]. In a semiclassical approach helium lines were calculated by Griem et al. [22, 23], using an impact approximation for electrons with a cutoff procedure, while almost stationary heavy ions are treated in a quasistatic ion approximation due to the static microfield. Also, molecular dynamics (MD) simulations have been performed by Calisti et al. [25] and Gigosos et al. [26] to include the influence of time-dependent microfield by introducing two kinds of simulations for calculating He I Stark line profiles.

Thermodynamic Green's function approach is a powerful tool to describe the Stark broadening [27–30]. In the last two decades, a quantum statistical approach has been developed, taking into account the medium effects by using Green's function [31–36]. In principle, this approach is able to describe dynamical screening and strong collisions by electrons, as well as the dynamic ion microfield, in a systematic way. This quantum statistical approach has been successfully applied to calculate the spectral line shapes of hydrogen, helium, H-, and He-like ions in dense plasmas [37–42].

In this paper thermodynamic Green's function approach is considered to calculate the pressure broadening of some selected neutral helium lines. In Section 2 the definitions and spectral properties of Green's function approach to spectral

line shapes of nonideal plasmas are presented. A review of the basic formalism is introduced and extended to helium lines. Section 3 provides the calculated shifts and full widths at half maximum (FWHM) for nonoverlapping, isolated (non-degenerate) He I lines 5048 Å ($2^1P - 4^1S$), 3889 Å ($2^3S - 3^3P$), and 3188 Å ($2^3S - 4^3P$) in dense plasmas. Finally, conclusions are given in Section 4.

2. Theoretical Calculations

Microscopic formation of the spectral line shapes in dense plasmas arises from perturbation of the radiative atom by collective and many-body effects [1, 4]. Thus, the interaction with the surrounding particles must be taken into account. For example, screening is considered as an important collective effect in plasmas. The influence of electrons and ions may be treated separately due to the difference in mass and mobility. Green's function methods provide a perturbative approach to correlation functions and quantum effects of many-body systems. Two-particle Green's function is used to calculate the line shape and electron broadening from the self-energy and the vertex function. From statistical properties of the system, the current-current correlations determine the absorption spectrum, which is utilized by Ross [27]. Recently, further improvements of this approach have been made by Röpke et al. [32], Hitzschke et al. [33], Günter et al. [34], and Omar et al. [41].

Optical properties of many-particle systems are specified by the dielectric function $\epsilon(\mathbf{q}, \omega)$ based on Green's function theory, which is the response of the medium to an external electromagnetic field. The longitudinal dielectric function is related to the polarization function $\Pi(\mathbf{q}, \omega)$

$$\epsilon_l(\mathbf{q}, \omega) = 1 - V(q)\Pi(\mathbf{q}, \omega), \quad (1)$$

where $V(q) = e^2/(\epsilon_0 q^2)$ is the Fourier transformed Coulomb potential. In terms of the absorption coefficient $\alpha(\omega)$ and the index of refraction $n(\omega)$, the transverse dielectric function $\epsilon_t(\mathbf{q}, \omega)$ in the long wavelength limit $q \rightarrow 0$ reads

$$\lim_{q \rightarrow 0} \epsilon_t(\mathbf{q}, \omega) = \left[n(\omega) + \frac{ic}{2\omega} \alpha(\omega) \right]^2. \quad (2)$$

In the visible region where the wavelength λ is large compared with the atomic dimension a_B , the transverse and the longitudinal part of dielectric function coincide. The absorption coefficient is proportional to the imaginary part of the dielectric function

$$\alpha(\omega) = \frac{\omega}{cn(\omega)} \lim_{q \rightarrow 0} \text{Im} \epsilon(\mathbf{q}, \omega),$$

$$n(\omega) = \frac{1}{\sqrt{2}} \lim_{q \rightarrow 0} \left\{ \text{Re} \epsilon(\mathbf{q}, \omega) + \left[(\text{Re} \epsilon(\mathbf{q}, \omega))^2 + \mathfrak{A} \right]^{1/2} \right\}^{1/2}, \quad (3)$$

where \mathfrak{A} denotes $(\text{Im} \epsilon(\mathbf{q}, \omega))^2$. In thermal equilibrium, the absorption coefficient is related to the emission coefficient by Kirchoff's law [43]. In optically thin plasma, the emission coefficient is proportional to the line emission. As mentioned

above, the dielectric function is related to the polarization function $\Pi(\mathbf{q}, \omega)$. Then the medium modifications of spectral line shapes can be addressed to the bound-bound two-particle polarization function, which concerns to dipole-dipole autocorrelation function [36].

The perturber-radiator interaction leads to pressure broadening, which contains electronic and ionic contributions. Describing the ionic contribution in the quasistatic approximation by averaging over the ionic microfield at radiating atom [31, 36, 44], we get

$$\begin{aligned} I^{\text{Pr}}(\omega) & \sim \sum_{i, i', f, f'} I_{i, i'}^{f, f'}(\omega) \int_0^\infty d\beta P(\beta) \\ & \times \text{Im} \left\langle i \left| \left\langle f \left| \left[\hbar\omega - \hbar\omega_{if} - \Sigma_{if}(\omega, \beta) + i\Gamma_{if}^{\text{V}} \right]^{-1} \right| f' \right\rangle \right| i' \right\rangle. \end{aligned} \quad (4)$$

Here, the ionic microfield distribution function $P(\beta)$ is taken according to the Hooper field distribution, and $\beta = E/E_0$ is the normalized field strength [45]. So $\hbar\omega_{if} = E_i - E_f$ is the unperturbed transition energy between the initial i and the final f states; i' and f' are the corresponding intermediate states

$$I_{i, i'}^{f, f'}(\omega) = \langle i | \mathbf{r} | f \rangle \langle f' | \mathbf{r} | i' \rangle \frac{\omega^4}{8\pi^3 c^3} e^{-\hbar\omega/k_B T}, \quad (5)$$

where $\langle i | \mathbf{r} | f \rangle$ is identified as a dipole matrix-element for the transition between i and f states. The line profile itself is determined by the vertex correction Γ_{if}^{V} for the overlapping lines and by the self-energy corrections Σ of the initial and final states

$$\begin{aligned} \Sigma_{if}(\omega, \beta) & = \text{Re} \left[\Sigma_i(\omega, \beta) - \Sigma_f(\omega, \beta) \right] \\ & + i \text{Im} \left[\Sigma_i(\omega, \beta) + \Sigma_f(\omega, \beta) \right]. \end{aligned} \quad (6)$$

Both electronic and ionic contributions occur in the self-energy $\Sigma_n(\omega, \beta)$, which is assumed to be diagonal in the atomic state n ;

$$\Sigma_n(\omega, \beta) = \Sigma_n^{\text{ion}}(\beta) + \Sigma_n^{\text{el}}(\omega, \beta). \quad (7)$$

The electronic self-energy is obtained by performing a Born approximation with respect to the perturber-radiator interaction [36]

$$\begin{aligned} \Delta_n^{\text{SE}} + i\Gamma_n^{\text{SE}} & = \left\langle n \left| \Sigma^{\text{el}}(E_n, \beta) \right| n \right\rangle \\ & = -\frac{1}{e^2} \int \frac{d^3 q}{(2\pi)^3} V(q) \sum_\alpha |M_{n\alpha}(\mathbf{q})|^2 \\ & \times \int_{-\infty}^\infty \frac{d\omega}{\pi} [1 + n_B(\omega)] \frac{\text{Im} \epsilon^{-1}(\mathbf{q}, \omega + i0)}{E_n - E_\alpha(\beta) - \hbar(\omega + i0)}. \end{aligned} \quad (8)$$

Here, the sum over α runs from $n-2$ to $n+2$ discrete bound states for virtual transitions, and the level splitting due to the

ion microfield $E_\alpha(\beta)$ has been neglected [35]. So $n_B(\omega) = [\exp(\hbar\omega/k_B T) - 1]^{-1}$ is the Bose distribution function, and $M_{n\alpha}(\mathbf{q})$ are the transition matrix-elements, given below. The inverse dielectric function $\varepsilon^{-1}(\mathbf{q}, \omega)$ contains many particle effects which account for the dynamical screening of the interaction in the plasma:

$$\text{Im } \varepsilon^{-1}(\mathbf{q}, \omega) = -\frac{\text{Im } \varepsilon(\mathbf{q}, \omega)}{[\text{Re } \varepsilon(\mathbf{q}, \omega)]^2 + [\text{Im } \varepsilon(\mathbf{q}, \omega)]^2}. \quad (9)$$

The random phase approximation (RPA) for the dielectric function is used:

$$\varepsilon^{\text{RPA}}(\mathbf{q}, \omega) = 1 - 2V(q) \int \frac{d^3 p}{(2\pi)^3} \frac{f_e(E_{\mathbf{p}}) - f_e(E_{\mathbf{p}+\mathbf{q}})}{E_{\mathbf{p}} - E_{\mathbf{p}+\mathbf{q}} - \hbar(\omega + i0)}. \quad (10)$$

where $E_{\mathbf{p}} = \hbar^2 \mathbf{p}^2 / 2m_e$ is the kinetic energy of electrons, and $f_e(E_{\mathbf{p}})$ is the Fermi distribution function of the electrons, approximated to the Boltzmann distribution function in the degenerate limit

$$f_e(E_{\mathbf{p}}) \simeq \frac{1}{2} n_e \left(\frac{2\pi\hbar^2}{m_e k_B T} \right)^{3/2} \exp\left(-\frac{\hbar^2 \mathbf{p}^2}{2m_e k_B T}\right). \quad (11)$$

The full expression of the inverse dielectric function has to be used if the transition frequency $\omega_{n\alpha}$ becomes comparable to the electron plasma frequency $\omega_{\text{pl}} = (n_e e^2 / \epsilon_0 m_e)^{1/2}$. However, in the high-frequency limit $\omega_{n\alpha} \gg \omega_{\text{pl}}$, the inverse dielectric function can be approximated by

$$\text{Im } \varepsilon^{-1}(\mathbf{q}, \omega) = \frac{-\text{Im } \varepsilon(\mathbf{q}, \omega)}{|\varepsilon(\mathbf{q}, \omega)|^2} \approx -\text{Im } \varepsilon(\mathbf{q}, \omega). \quad (12)$$

This binary collision approximation leads to a linear behavior of the electronic shift with respect to the electron density, whereas a nonlinear dependence of the electronic shift with increasing electron density is expected if the full expression of the inverse dielectric function is used [33, 35].

The vertex function for the coupling between the upper and the lower state is given by

$$\Gamma_{if}^V = \frac{2\pi}{e^2} \int \frac{d^3 q}{(2\pi)^3} \frac{d^3 p}{(2\pi)^3} f_e(E_{\mathbf{p}}) V^2 \times (q) M_{ii}(\mathbf{q}) M_{ff}(-\mathbf{q}) \delta\left(\frac{\hbar^2 \mathbf{p} \cdot \mathbf{q}}{m_e}\right). \quad (13)$$

The transition matrix-elements $M_{n\alpha}(\mathbf{q})$ describe the coupling between free charges and bound states. In lowest order, they are determined by the atomic eigenfunctions $\psi_n(\mathbf{p})$ of the radiating electron and depend on the momentum transfer $\hbar\mathbf{q}$ [34, 46]

$$M_{n\alpha}(\mathbf{q}) = \int \frac{d^3 p}{(2\pi)^3} \psi_n^*(\mathbf{p}) \times \left[Z e \psi_\alpha\left(\mathbf{p} - \frac{m_e}{m_i + m_e} \mathbf{q}\right) - e \psi_\alpha\left(\mathbf{p} + \frac{m_i}{m_i + m_e} \mathbf{q}\right) \right], \quad (14)$$

assuming that the ion with charge Z is much heavier than the electron $m_i \gg m_e$:

$$M_{n\alpha}(\mathbf{q}) = \int \frac{d^3 p}{(2\pi)^3} \psi_n^*(\mathbf{p}) [Z e \psi_\alpha(\mathbf{p}) - e \psi_\alpha(\mathbf{p} + \mathbf{q})] = i e \left(Z \delta_{n\alpha} - \int d^3 r \psi_n^*(\mathbf{r}) \exp(i\mathbf{q} \cdot \mathbf{r}) \psi_\alpha(\mathbf{r}) \right). \quad (15)$$

Expanding the plane wave into spherical harmonics

$$\exp(i\mathbf{q} \cdot \mathbf{r}) = 4\pi \sum_{l=0}^{\infty} \sum_{m=-l}^l i^l j_l(qr) Y_{lm}^*(\Omega_q) Y_{lm}(\Omega_r), \quad (16)$$

where $j_l(qr)$ is the Bessel function, a multipole expansion can be derived; for example, $l = 0, 1, 2$ gives the monopole, dipole, and quadrupole contribution of the radiator-electron interaction, respectively. The radial part of helium wave function is calculated based on Coulomb approximation method of Bates and Damgaard [47–49]. For more detail see [41].

By using the Born approximation, the electronic self-energy is overestimated. To avoid this we apply a cutoff procedure and add the strong collision term in contrast to partial summation of the three-particle T-matrix, which is quite suitable for treating short-range interactions between particles [50], where the result might be slightly modified. According to Griem, the cutoff parameter for the q -integration is the inverse of the minimum limiting impact parameter ($q_{\text{max}} = 1/\rho_{\text{min}}$) [22, 36, 49, 51].

To determine the ionic self-energy, we approximate the time-dependent microfield fluctuation by its static value. In general, dynamic ionic microfield is important for overlapping lines and at low electron density in the line center [52, 53]. Due to the slow movement of heavy ions, the ion microfield is assumed to be constant during the time of interest for the radiation process. The static ionic contribution to the ionic self-energy is treated by means of the microfield concept including both quadratic Stark effect and quadrupole effects. The first-order perturbation term vanishes for nonhydrogenic like atoms because of nondegeneracy with respect to the orbital quantum number l . According to second-order perturbation theory, the quadratic Stark effect is proportional to the square of the microfield [54]

$$\Sigma_{nlm}^2(E) = e^2 |E|^2 \sum_{n', l', m'} \frac{|\langle n, l, m | z | n', l', m' \rangle|^2}{E_{nlm} - E_{n'l'm'}}, \quad (17)$$

where E is the microfield strength; n , l , and m are the well-known principal, orbital, and magnetic atomic quantum numbers, respectively. The quadrupole Stark effect is due to the inhomogeneity of the ionic microfield. We use the expression derived by Halenka [55]:

$$\Sigma_{nn'}^3(E) = -\frac{5}{2\sqrt{3}2\pi} \frac{eE_0}{r_0} B_\rho(\beta) \langle n | 3z^2 - r^2 | n' \rangle. \quad (18)$$

Here, $B_\rho(\beta)$ is the mean field gradient at a given field strength, and the screening parameter $\rho = r_0/r_D$ is taken as the ratio between the mean particles distance r_0 and the Debye radius r_D .

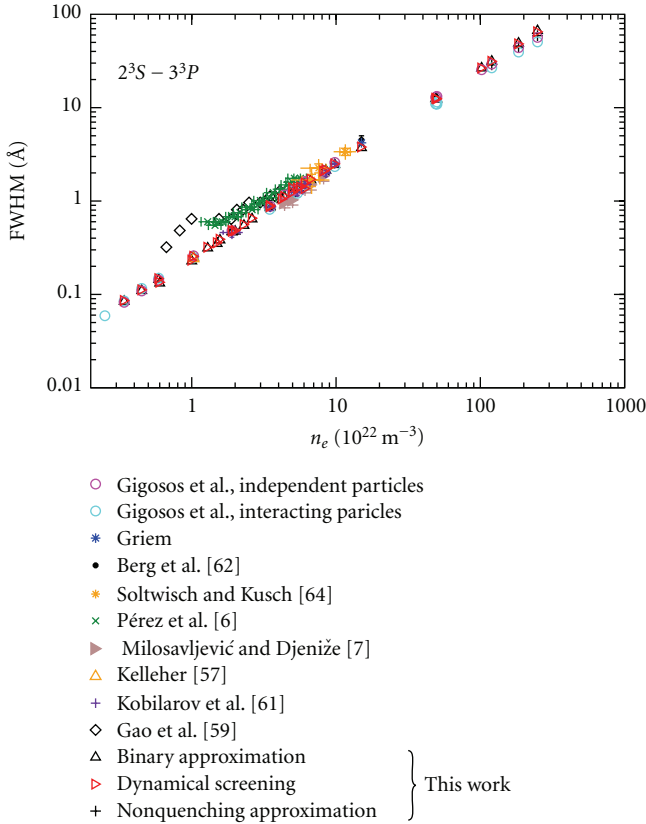


FIGURE 1: Stark FWHM for the He I line 3889 Å as a function of electron density. A comparison is made with the measured [6, 56–61] and other theoretical data [22, 62].

3. Results and Discussions

The Stark broadening parameters for the transition ($2^1P - 4^1S$) 5048 Å are given in Table 1. Our width w and shift d results are compared to calculated values of Bassalo et al. (BCW) [66], measurements of Kelleher [56], and measurements of Diatta [67]. Our calculations agree better with the measured value by Kelleher [56] in contrast to the results given by Bassalo et al. [66]. The measured shift by Diatta [67] is obviously smaller than the calculated shifts given in Table 1.

The Stark width and shift of the line ($2^3S - 3^3P$) 3889 Å are measured by Pérez et al. [6]. The measured values were in the plasma density range of $(1 - 6) \times 10^{22} \text{ m}^{-3}$ and temperature interval of $(0.8 - 3) \times 10^4 \text{ K}$ with a mean value of $2 \times 10^4 \text{ K}$. The error bar in the case of n_e was $\pm 10\%$, and the uncertainty in the temperature evaluation was about 20%. Recently, the FWHM of this line is measured by Gao et al. [61] for a helium arc for density range $(0.5 - 4) \times 10^{22} \text{ m}^{-3}$. Figures 1 and 2 include other available experimental [56–60, 63] and theoretical results [22, 62]. The MD simulation results of Gigosos et al. [62] have been performed for independent as well as interacting particles in nonquenching approximation. Our calculations are also presented, the width shows a good agreement especially with the MD simulations data of Gigosos et al. [62], where no Doppler

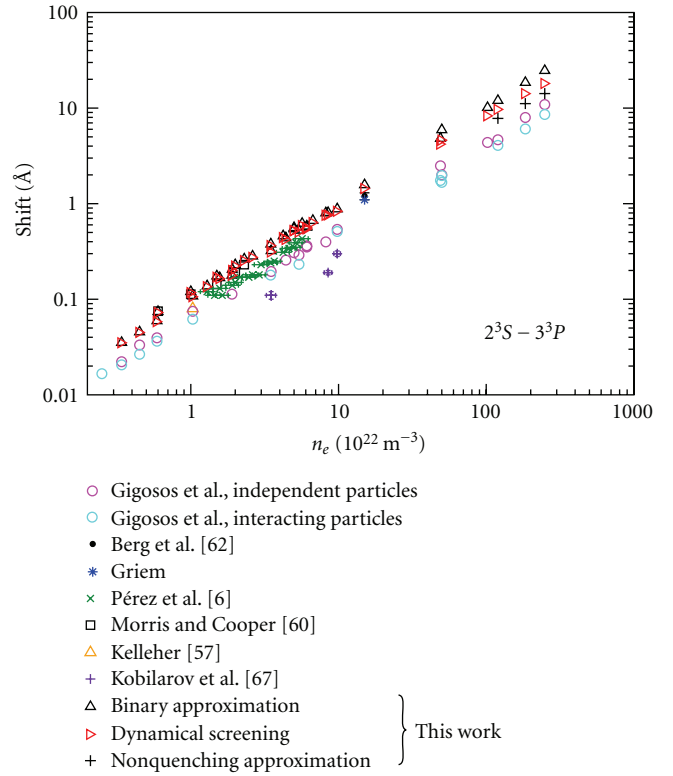


FIGURE 2: Stark shift for the He I line 3889 Å as a function of electron density. A comparison is made with the measured [6, 56–58, 63] and other theoretical data [22, 62].

broadening is included. Nonlinearity can be seen at very high electron density. The discrepancy between the measured and calculated line broadening may be related to self absorption [61]. However, our results for the shift are overestimated, on the other hand better agreement can be seen by comparing our results in non-quenching approximation with the results of Gigosos et al. [62], which give lower values of shift at high electron density.

The Stark parameters of the line ($2^3S - 4^3P$) 3188 Å are measured by Peláez et al. [64]. They made a spectroscopic and interferometric analysis of a pulsed plasma. The electron temperature (from 1900 K to 2300 K) was obtained from the intensity ratio of He II lines. Electron density was determined by interferometry, ranging from $1.25 \times 10^{22} \text{ m}^{-3}$ to $6.22 \times 10^{22} \text{ m}^{-3}$. From these experimental results an empirical calibration for the Stark parameters was obtained in a broad range of electron densities [64]. The experimental and various theoretical Stark parameters are reported by Peláez et al. [64], and our results are included in Figures 3 and 4 for Stark width and shift as a function of electron density, respectively, at the given plasma temperatures. Theoretical predictions of Bassalo et al. (BCW) [24] can also be seen in Figures 3 and 4. Further experimental results are presented, carried out by Kelleher [56], Mijatović et al. [65], Berg et al. [58], and Soltwisch and Kusch [60]. The measured value of Berg et al. [58] was compared with Griem's theory [58]

TABLE 1: The calculated FWHM and shift (without/with screening) for the line 5048 Å are given; w_{th} and d_{th} this work; w_{B} and d_{B} Bassalo et al. [66]. The experimental w_{exp} and d_{exp} are included [56, 67].

n_e (10^{22} m^{-3})	T_e (10^3 K)	w_{B} (Å)	w_{th} (Å)	w_{exp} (Å)	d_{B} (Å)	d_{th} (Å)	d_{exp} (Å)
3.2	30.0	5.22/5.22	5.385/5.378	—	2.19/2.05	2.56/2.397	—
2.0	18.0	3.10/3.10	3.183/3.179	3.4	1.43/1.35	1.783/1.677	0.9 [67]
$1.03 \pm 12\%$	$20.9 \pm 20\%$	1.58/1.58	1.623/1.622	1.68	0.75/0.68	0.862/0.82	0.89 [56]

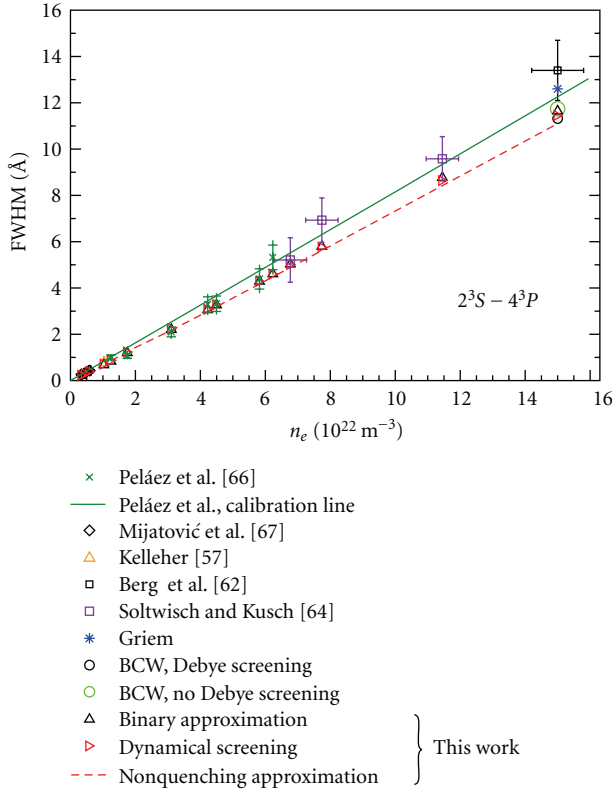


FIGURE 3: The measured Stark FWHM and calculated values for He I 3188 Å line versus electron density. The calculated Stark widths are included from different approaches [22, 24, 56, 58, 60, 64, 65].

at electron density $(1.5 \pm 0.08) \times 10^{23} \text{ m}^{-3}$ and temperature $(2.9 \pm 0.2) \times 10^4 \text{ K}$.

4. Conclusions

The quantum statistical approach has been developed to calculate spectral line shapes in dense plasmas. By using thermodynamic Green's function, a systematic perturbative treatment of the polarization function has been performed [33, 34, 46]. In contrast to the molecular dynamics (MD) simulations, consistent quantum description is applied here to calculate the Stark parameters by using the formalism presented above. The calculated Stark shift and full width at half maximum (FWHM) of He I lines 5048 Å ($2^1P - 4^1S$), 3889 Å ($2^3S - 3^3P$), and 3188 Å ($2^3S - 4^3P$) have been calculated in the density range $(10^{21} - 10^{24}) \text{ m}^{-3}$ and for temperatures between $(0.5 - 6) \times 10^4 \text{ K}$. In dense plasmas the *binary (few-particle) collision approximation*

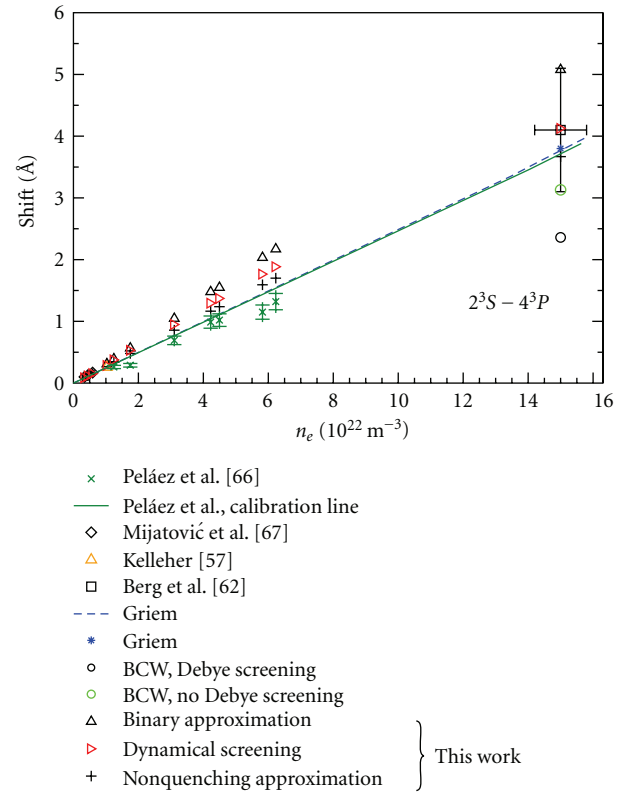


FIGURE 4: The measured Stark shift and calculated values for He I 3188 Å line versus electron density. The calculated Stark shifts are included from different theoretical approaches [22, 24, 56, 58, 64, 65].

is not appropriate to describe the collective interactions; therefore at high densities the *dynamical screening effect* will be more important seen (12), which reduces the linearity of Stark parameters with increasing electron density. This affects mostly the shift than the width, and it can be seen in Figures 2 and 4. The Hooper microfield distribution function is applicable for plasmas in the regime $\Gamma \leq 1$, in which the correlations between plasma particles are considered as small perturbations. This distribution is not applicable in strongly coupling regime, where the correlation effect is important at high density, and therefore a new distribution function should be adopted. Generally, our calculated line widths show good agreement by comparing with other results, while the shift is slightly overestimated for the lines 3889 Å and 3188 Å. However, by performing *nonquenching approximation* better agreement can be seen.

Moreover, our quantum statistical approaches can be applied not only to investigate the line shapes of two-electron atom but also to complex atoms. Furthermore, the deformation of spectral line profiles can be investigated in a strong magnetic field for stellar diagnostic.

Acknowledgments

This project is supported by Emmy Noether-Program of the Deutsche Forschungsgemeinschaft, RE1141/11-1. The author would like to thank A. Wierling, G. Röpke, and M. A. Gonzalez for helpful discussions.

References

- [1] H. R. Griem, *Principles of Plasma Spectroscopy*, Cambridge University Press, Cambridge, UK, 1997.
- [2] W. Lochte-Holtgreven, *Plasma Diagnostics*, American Institute of Physics, New York, NY, USA, 1995.
- [3] T. Fujimoto, *Plasma Spectroscopy*, Clarendon Press, Oxford, UK, 2004.
- [4] G. W. Collins, *The Fundamentals of Stellar Astrophysics*, W. H. Freeman, New York, NY, USA, 1989.
- [5] C. Pérez, I. de la Rosa, A. M. de Frutos, and S. Mar, "Calibration of the Stark-broadening parameters for some He I lines," *Physical Review A*, vol. 44, no. 10, pp. 6785–6790, 1991.
- [6] C. Pérez, R. Santamarta, M. I. de la Rosa, and S. Mar, "Stark broadening of neutral helium lines and spectroscopic diagnostics of pulsed helium plasma," *European Physical Journal D*, vol. 27, no. 1, pp. 73–75, 2003.
- [7] V. Milosavljević and S. Djenize, "Ion contribution to the astrophysical important 447.15, 587.56 and 667.82 nm He I spectral lines broadening," *Astronomy and Astrophysics*, vol. 393, no. 2, pp. 721–726, 2002.
- [8] A. Beauchamp, F. Wesemael, and P. Bergeron, "Spectroscopic studies of DB white dwarfs: improved stark profiles for optical transitions of neutral helium," *Astrophysical Journal, Supplement Series*, vol. 108, no. 2, pp. 559–573, 1997.
- [9] M. S. Dimitrijević and S. Sahal-Bréchet, "Stark broadening of neutral helium lines," *Journal of Quantitative Spectroscopy and Radiative Transfer*, vol. 31, no. 4, pp. 301–313, 1984.
- [10] M. Koubiti, H. Capes, L. Mouret, et al., "Density diagnostic using Stark broadening of HeI spectral line emission from Rydberg levels," in *Proceedings of the Workshop on Privacy Enhancing Technologies (PET '05)*, Forschungszentrum Jülich GmbH, Cavtat, Croatia, October 2005.
- [11] A. C. Kolb and H. Griem, "Theory of line broadening in multiplet spectra," *Physical Review*, vol. 111, no. 2, pp. 514–521, 1958.
- [12] M. Baranger, in *Atomic and Molecular Processes*, D. R. Bates, Ed., chapter 13, Academic Press, New York, USA, 1962.
- [13] H. Margenau and M. Lewis, "Structure of spectral lines from plasmas," *Reviews of Modern Physics*, vol. 31, no. 3, pp. 569–615, 1959.
- [14] E. W. Smith, J. Cooper, and C. R. Vidal, "Unified classical-path treatment of stark broadening in plasmas," *Physical Review*, vol. 185, no. 1, pp. 140–151, 1969.
- [15] R. W. Lee, "Plasma line shapes for selected transitions in hydrogen-, helium- and lithium-like ions," *Journal of Quantitative Spectroscopy and Radiative Transfer*, vol. 40, no. 5, pp. 561–568, 1988.
- [16] M. Baranger, "General impact theory of pressure broadening," *Physical Review*, vol. 112, no. 3, pp. 855–865, 1958.
- [17] D. Voslamber, "Unified quantum statistical formulation of pressure broadening," *Physics Letters A*, vol. 40, no. 3, pp. 266–268, 1972.
- [18] T. Hussey, J. W. Dufty, and C. F. Hooper Jr., "Kinetic theory of spectral line broadening," *Physical Review A*, vol. 12, no. 3, pp. 1084–1093, 1975.
- [19] D. B. Boercker and J. W. Dufty, "Quantum kinetic theory of time-correlation functions," *Physical Review A*, vol. 23, no. 4, pp. 1952–1968, 1981.
- [20] H. Nguyen, M. König, D. Benredjem, M. Caby, and G. Coulaud, "Atomic structure and polarization line shift in dense and hot plasmas," *Physical Review A*, vol. 33, no. 2, pp. 1279–1290, 1986.
- [21] S. Günter, "Stark Shift and Broadening of Hydrogen Spectral Lines," *Contributions to Plasma Physics*, vol. 29, p. 479, 1989.
- [22] H. R. Griem, *Spectral Line Broadening by Plasmas*, Academic Press, New York, NY, USA, 1974.
- [23] H. R. Griem, M. Baranger, A. C. Kolb, and G. Oertel, "Stark broadening of neutral helium lines in a plasma," *Physical Review*, vol. 125, no. 1, pp. 177–195, 1962.
- [24] J. M. Bassalo, M. Cattani, and V. S. Walder, "Convergent calculations for electron impact broadening and shift of neutral helium lines," *Journal of Quantitative Spectroscopy and Radiative Transfer*, vol. 28, no. 2, pp. 75–80, 1982.
- [25] A. Calisti, R. Stamm, and B. Talin, "Simulation calculation of the ion-dynamic effect on overlapping neutral helium lines," *Physical Review A*, vol. 38, no. 9, pp. 4883–4886, 1988.
- [26] M. A. Gigoso, M. A. Gonzalez, B. Talin, and A. Calisti, "Molecular Dynamics Simulations of He I Stark broadened Line Profiles," in *Proceedings of the 17th International Conference on Spectral Line Shapes*, E. Dalimier, Ed., p. 451, Frontier Group, Paris, France, 2004.
- [27] D. W. Ross, "Pressure broadening as a many-body problem," *Annals of Physics*, vol. 36, no. 3, pp. 458–485, 1966.
- [28] H. R. Zaidi, "Calculation of resonance broadening," *Physical Review*, vol. 173, no. 1, pp. 123–132, 1968.
- [29] B. Bezzerides, "Radiation absorption phenomena in gases-I general theory of line broadening," *Journal of Quantitative Spectroscopy and Radiative Transfer*, vol. 7, no. 2, pp. 353–371, 1967.
- [30] B. Bezzerides, "Resonance broadening of absorption lines," *Physical Review*, vol. 159, no. 1, pp. 3–10, 1967.
- [31] G. Röpke and L. Hitzschke, "Shift and Broadening of Spectral Lines in Non-ideal Plasmas," in *Proceedings of the 9th International Conference on Spectral Line Shapes*, J. Szudy, Ed., p. 49, Ossolineum, Waroclaw, Poland, 1989.
- [32] G. Röpke, T. Seifert, and K. Kilimann, "A Green's Function Approach to the Shift of Spectral lines in Dense Plasmas," *Annalen der Physik (Leipzig)*, vol. 38, p. 381, 1981.
- [33] L. Hitzschke, G. Röpke, T. Seifert, and R. Zimmermann, "Green's function approach to the electron shift and broadening of spectral lines in non-ideal plasmas," *Journal of Physics B*, vol. 19, no. 16, pp. 2443–2456, 1986.
- [34] S. Günter, L. Hitzschke, and G. Röpke, "Hydrogen spectral lines with the inclusion of dense-plasma effects," *Physical Review A*, vol. 44, no. 10, pp. 6834–6844, 1991.
- [35] S. Günter and A. Könies, "Quantum mechanical electronic width and shift of spectral lines over the full line profile-Electronic asymmetry," *Journal of Quantitative Spectroscopy and Radiative Transfer*, vol. 52, no. 6, pp. 819–824, 1994.
- [36] S. Günter, "Optische Eigenschaften dichter Plasmen," Habilitation thesis, Rostock University, Rostock, Germany, 1996, IPP MPI no. 5/67.

- [37] St. Böddeker, S. Günter, A. Könies, L. Hitzschke, and H.-J. Kunze, "Shift and width of the H_{α} line of hydrogen in dense plasmas," *Physical Review E*, vol. 47, no. 4, pp. 2785–2791, 1993.
- [38] A. Döhrn, P. Nowack, A. Könies, S. Günter, and V. Helbig, "Stark broadening and shift of the first two Paschen lines of hydrogen," *Physical Review E*, vol. 53, no. 6, pp. 6389–6395, 1996.
- [39] S. Günter and A. Könies, "Shifts and asymmetry parameters of hydrogen Balmer lines in dense plasmas," *Physical Review E*, vol. 55, no. 1, pp. 907–911, 1997.
- [40] B. Omar, A. Wierling, S. Günter, and G. Röpke, "Hydrogen Balmer spectrum from a high-pressure arc discharge: revisited," *Contributions to Plasma Physics*, vol. 47, no. 4-5, pp. 315–323, 2007.
- [41] B. Omar, S. Günter, A. Wierling, and G. Röpke, "Neutral helium spectral lines in dense plasmas," *Physical Review E*, vol. 73, no. 5, Article ID 056405, 2006.
- [42] B. Omar, A. Wierling, S. Günter, and G. Röpke, "Analysing brilliance spectra of a laser-induced carbon plasma," *Journal of Physics A*, vol. 39, no. 17, pp. 4731–4737, 2006.
- [43] G. A. Kobzev, I. T. Yakubov, and M. M. Popovich, Eds., *Transport and Optical Properties of Nonideal Plasmas*, Plenum Press, New York, NY, USA, 1995.
- [44] S. Sorge, A. Wierling, G. Röpke, W. Theobald, R. Sauerbrey, and T. Wilhein, "Diagnostics of a laser-induced dense plasma by hydrogen-like carbon spectra," *Journal of Physics B*, vol. 33, no. 16, pp. 2983–3000, 2000.
- [45] C. F. Hooper Jr., "Low-frequency component electric microfield distributions in plasmas," *Physical Review*, vol. 165, no. 1, pp. 215–222, 1968.
- [46] W.-D. Kraeft, D. Kremp, W. Ebeling, and G. Röpke, *Quantum Statistics of Charged Particle Systems*, Akademie, Berlin, Germany, 1986.
- [47] D. R. Bates and A. Damgaard, "The Calculation of the Absolute Strengths of Spectral Lines," *Philosophical Transactions of the Royal Society A*, vol. 242, p. 101, 1949.
- [48] I. I. Sobel'mann, *Atomic Spectra and Radiative Transitions*, Springer, Berlin, Germany, 1992.
- [49] H. R. Griem, "Stark broadening of isolated spectral lines from heavy elements in a plasma," *Physical Review*, vol. 128, no. 2, pp. 515–523, 1962.
- [50] V. G. Morozov and G. Röpke, "The "Mixed" Green's Function Approach to Quantum Kinetics with Initial Correlations," *Annals of Physics*, vol. 278, p. 127, 1999.
- [51] H. R. Griem and C. S. Shen, "Application of a dispersion relation to the electron impact widths and shifts of isolated spectral lines from neutral atoms," *Physical Review*, vol. 125, no. 1, pp. 196–199, 1962.
- [52] G. Röpke, S. Sorge, and A. Wierling, "Line profiles in dense plasmas: dynamical microfield, radiation transport," *Contributions to Plasma Physics*, vol. 41, no. 2-3, pp. 187–190, 2000.
- [53] S. Sorge, S. Günter, and G. Röpke, "On the consequences of a realistic conditional covariance in MMM-calculations," *Journal of Physics B*, vol. 32, no. 3, pp. 675–681, 1999.
- [54] H. A. Bethe and E. E. Salpeter, *Quantum Mechanics of One- and Two-Electron Atoms*, Plenum, New York, NY, USA, 1977.
- [55] J. Halenka, "Asymmetry of hydrogen lines in plasmas utilizing a statistical description of ion-quadruple interaction in Mozer-Baranger limit," *Zeitschrift für Physik D*, vol. 16, no. 1, pp. 1–8, 1990.
- [56] D. E. Kelleher, "Stark broadening of visible neutral helium lines in a plasma," *Journal of Quantitative Spectroscopy and Radiative Transfer*, vol. 25, no. 3, pp. 191–220, 1981.
- [57] R. Kobilarov, N. Konjević, and M. V. Popović, "Influence of ion dynamics on the width and shift of isolated He I lines in plasmas," *Physical Review A*, vol. 40, no. 7, pp. 3871–3879, 1989.
- [58] H. F. Berg, A. W. Ali, R. Lincke, and H. R. Griem, "Measurement of stark profiles of neutral and ionized helium and hydrogen lines from shock-heated plasmas in electromagnetic T tubes," *Physical Review*, vol. 125, no. 1, pp. 199–206, 1962.
- [59] V. Milosavljević and S. Djeniže, "Ion contribution to the astrophysical important 388.86, 471.32 and 501.56 nm He I spectral lines broadening," *New Astronomy*, vol. 7, p. 543, 2002.
- [60] H. Soltwisch and H. J. Kusch, "Experimental Stark profile Determination of some Plasma Broadened He I- and He II-Lines," *Zeitschrift für Naturforschung A*, vol. 34, p. 300, 1979.
- [61] H. M. Gao, S. L. Ma, C. M. Xu, and L. Wu, "Measurements of electron density and Stark width of neutral helium lines in a helium arc plasma," *European Physical Journal D*, vol. 47, no. 2, pp. 191–196, 2008.
- [62] M. A. Gigosos, M. A. Gonzalez, B. Talin, and A. Calisiti, private communications.
- [63] R. N. Morris and J. Cooper, "Stark Shifts of He I 3889, He I 4713, and He I 5016," *Canadian Journal of Physics*, vol. 51, p. 1746, 1973.
- [64] R. J. Peláez, V. R. Gonzalez, F. Rodriguez, J. A. Aparicio, and S. Mar, "Stark parameters of neutral helium 318.8 nm line," *Astronomy and Astrophysics*, vol. 453, no. 2, pp. 751–754, 2006.
- [65] Z. Mijatović, N. Konjević, M. Ivković, and R. Kobilarov, "Influence of ion dynamics on the width and shift of isolated He I lines in plasmas. II," *Physical Review E*, vol. 51, no. 5, pp. 4891–4896, 1995.
- [66] J. M. Bassalo, M. Cattani, and V. S. Walder, "Semiclassical convergent calculations for the electron-impact broadening and shift of some lines of neutral helium in a hot plasma," *Physical Review A*, vol. 22, no. 3, pp. 1194–1197, 1980.
- [67] C. S. Diatta, Ph.D. thesis, University d'Orleans, Orleans, France, 1977.



Hindawi

Submit your manuscripts at
<http://www.hindawi.com>

